Available online at www.sciencedirect.com
SCIENCE DIRECT
Polymer 47 (2006) 1414–1422
polymer
www.elsevier.com/locate/polymer

Intermolecular interactions and formation of the hydration sphere in phosphonic acid model systems as an approach to the description of vinyl phosphonic acid based polymers

Robson Pacheco Pereira [a], Maria Isabel Felisberti [b], Ana Maria Rocco [a,*]

[a] Grupo de Materiais Condutores e Energia, Instituto de Química, Universidade Federal do Rio de Janeiro, 21941-970 Rio de Janeiro, RJ, Brazil
[b] Grupo de Pesquisa em Polímeros, Instituto de Química, UNICAMP, 13083-970 Campinas, SP, Brazil

Received 7 November 2005; received in revised form 14 December 2005; accepted 15 December 2005
Available online 18 January 2006

Abstract

Molecular model systems based on propyl phosphonic acid (ppa) were studied by means of density functional theory calculations in order to describe the acid–acid interaction and the formation of the hydration sphere. The formation of ppa dimers is reported and the energetic difference between two dimer structures is presented. The hydration sphere of ppa was represented by model systems ppa$(H_2O)_n$, for which the system with $n=4$ formed the first hydration sphere (h^1), while $n=7$ can be considered a good approximation to the complete inner hydration sphere around the phosphonic acid group. The study of the ppa–H^+ $(H_2O)_n$ model systems showed an interesting structural behavior comparatively to the ppa$(H_2O)_n$ systems. The protonated acids exhibited equivalent phosphorous–oxygen bonds and a general molecular structure is proposed to represent these protonated species.

Keywords: Phosphonic acid; Hydration sphere; DFT calculations

1. Introduction

Fuel cells (FC) are devices in which the chemical energy is converted into electrical energy to be used as power source in houses, distributed power plants and electric vehicles [1]. FC are formed by the assembly of three components: cathode, electrolyte and anode. Optimization of electrolyte materials for application in FC is required in order to substitute the most common membranes commercially used by other with higher efficiency. Different polymer electrolytes for FC have been developed and tested, dependent, obviously, on the type of fuel to be employed. Among the cells already developed are the alkaline fuel cell (AFC), the proton exchange membrane fuel cell (PEMFC), the phosphoric acid fuel cell (PAFC), the molten carbonate fuel cell (MCFC), the solid oxide fuel cell (SOFC) and the direct methanol fuel cell (DMFC) [2].

In PEMFC devices, the electrolyte employed is usually a proton-conducting membrane, and many systems have been reported in the literature, including polybenzimidazole-based electrolytes [3], sulfonated membranes [4] and, more recently, anion-conducting membranes for direct methanol fuel cells [5]. Most of the PEMFC related in the literature use a commercial proton exchange membrane such as DOW® (DOW Chemicals), Flemion® (Asashi Glass) and NAFION® (DuPont) [6,7]. Utilisation of these materials, however, impose restrictions in the temperature range of the PEMFC operation from 50 to 125 °C [8]. Additionally, proton mobility decreases strongly with dehydration at high temperatures due to the chemical structure of the chain backbone [9]. The knowledge of the proton conduction mechanisms and the nanostructure of polymer membranes is important to establish the molecular architecture and the nanostructure of optimized polymer electrolytes [10].

The design and synthesis of new membranes possessing improved performance characteristics (along with decreased manufacturing costs) will require a fundamental, molecular based understanding of the mechanisms of proton and water transport as a function of membrane hydration, morphology, and polymer chemistry. This information cannot come from experimental investigations alone, but will require knowledge of how membrane morphology and chemical composition affect the transport of both protons and water in the PEM through multiscale modeling that bridges many distinct time

* Corresponding author. Fax: +55 21 2562 7559.
E-mail address: amrocco@iq.ufrj.br (A.M. Rocco).

0032-3861/$ - see front matter © 2005 Elsevier Ltd. All rights reserved.
doi:10.1016/j.polymer.2005.12.034

and length scales, connecting the equilibrium conformational structure of a membrane and its general composition to molecular processes including proton dissociation, transfer, and diffusion, and hydrogen bonding, distribution, and diffusion of water [11,12].

Phosphonic acid-based polymers have been synthesized earlier aiming applications such as cation-exchange membranes for specific cation binding and removal [13] and fuel cell membranes [14]. More specifically, poly(styrene-*co*-vinyl phosphonic acid) ionomers were synthesized and characterized by Wu and Weiss [15], via hydrolysis of poly(styrene-*co*-diethyl vinyl phosphonate). In their work, authors observed a lower glass transition temperature (T_g) for the phosphonate ester, and a higher T_g for the phosphonic acid derivative, in comparison with polystyrene. Wu and Weiss also described a small water absorption and a non-conductive behavior for the membranes studied, and attributed this last feature to the possibility of hydrogen bonding self-association among the acid groups, which would lead to a few phosphonic acid sites available for hydrogen bonding with water.

DFT calculations are employed in the present work to describe the formation of the hydration sphere around the phosphonic acid group, the acid–acid interactions (formation of acid dimers) and the proton–acid interaction. This theoretical approach aims to help on the molecular description of vinyl phosphonic acid based polymers.

2. Calculation details

Density functional theory calculations (DFT) were carried out on the model systems based on propyl phosphonic acid (ppa), shown in Fig. 1. The formation of the hydration sphere was studied in model systems ppa$(H_2O)_n$, for n between 1 and 7. The calculations were performed with the 6-31G(d,p) standard basis sets for all atoms, along with the gradient corrected DFT method, Becke3-Lee-Yang-Parr, (B3LYP) [16]. In order to investigate the behavior of the total energy for the present system with a higher number of water molecules, geometry optimization calculations were carried out on model systems ppa$(H_2O)_{14}$ and ppa$(H_2O)_{28}$ with 3-21G basis set and, for the optimized structures, a single point calculation with the 6-31G(d,p) basis set was performed. Geometry optimization calculations were also carried out for ppa–$H^+(H_2O)_n$ model systems, with the 6-31G(d,p) basis set and the gradient corrected DFT method, B3LYP. All the calculations were carried out using the GAMESS code [17].

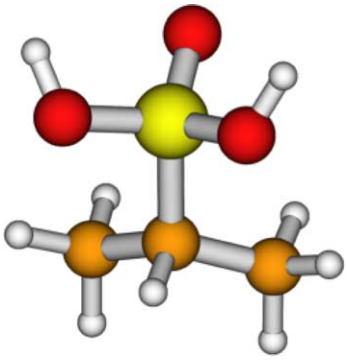

Fig. 1. Molecular structure of propyl phosphonic acid (ppa).

3. Results and discussion

3.1. Molecular geometry of propyl phosphonic acid (ppa)

The molecular models for acid dimers are shown in Fig. 2 and selected geometrical parameters are shown in Table 1 for propyl phosphonic acid (ppa) and the acid dimers with two and three hydrogen bond sites.

The comparison of the structural parameters calculated in the present work with those obtained experimentally by Weakley [18,19] allows the identification of a good agreement for the phosphonic acid group, especially the C–P and P=O bonds. Weakley found a C–P bond length of 1.817 Å, while the DFT calculations indicated 1.82441 Å; the experimental value found for P=O was 1.455 Å and the theoretical description in the present work resulted in 1.49209 Å for this bond. The overestimated value of the P=O bond length is probably associated with the acid–acid interactions in solid state, where the molecular and electronic structure are strongly influenced by these interactions.

In order to describe the acid–acid interactions, three model systems were tested with 1, 2 or 3 hydrogen bonding sites. The full geometry optimization of such systems lead to only two molecular structures, as shown in Fig. 2. The model system with one hydrogen bonding site relaxed by rotation over the hydrogen bonding axis to a system with two interaction sites. Increasing the number of hydrogen bonds from 2 to 3 increases the stabilization of the system in 0.172 hartree (about 106 kcal mol^{-1}).

From Table 1, it can be seen a small variation in the C–P bond length, when the isolated acid and the dimers are compared, while the bond lengths involving P, O and H (in the acid group) exhibit a higher sensibility to formation of dimers as well as the geometry of the interaction. The symmetry of the interaction strongly influences the geometrical parameters, such as the bond lengths and angles, listed in Table 1, where a differentiation between the hydroxyl groups acting as acid and base in the system is evident.

P=O length exhibited an increase of 1.4% comparing the isolated ppa and $(ppa)_2$(b), evidencing a decrease in the electronic density in this bond, due to the interaction with the acid group in the other ppa unit. The length relative to the P–O bond presented two distinct behaviors, depending on the acid or basic characteristic of the interaction involved. In $(ppa)_2$(a), one of the hydroxyl groups acts as base in the interaction and d(P–O) increases from 1.63226 to 1.66322 Å, with an obvious decrease in the electronic density in the P–O bond. Simultaneously, the other hydroxyl group acts as an acid and, for this one, d(P–O) decreases to 1.57757 Å. In the model system $(ppa)_2$(b), both OH groups act as acids, and d(P–O) decreases to 1.58667 Å.

The B3LYP correlation–exchange functional has been widely used in the literature, aiming the study of molecular

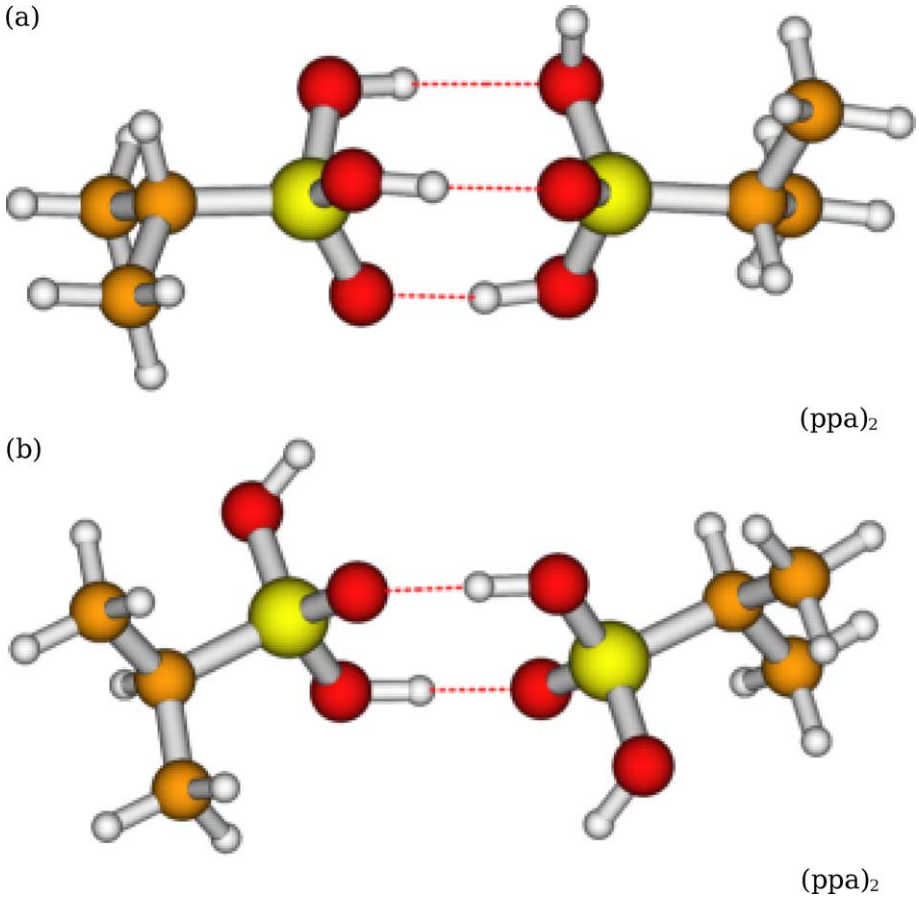

Fig. 2. Molecular structure of acid dimers involving (a) three sites of interaction and (b) two sites of interaction.

geometries, electronic states and vibrational spectra [20]. This hybrid functional, as mentioned by other authors [21] present very good agreement with experimental data, depending, obviously, on the molecular model chosen to represent the experimental system. In cases where interactions other than intramolecular play an important role in the molecular system, bond lengths may be overestimated, as observed by Zhang and co-workers [22].

3.2. Formation of the hydration sphere in ppa(H_2O)$_n$ systems

Since polymer membranes usually operate in FC devices under humidification, in order to give appreciable conductivity values, the formation of the hydration sphere was calculated aiming the comparison with experimental data of water uptake. Different model systems based on the propyl phosphonic acid with increasing number of water molecules, from 1 to 7, were studied in DFT geometry optimization calculations. The total energy of these systems was evaluated as a function of the number of water molecules in the hydration sphere, as well as the changes in the molecular geometry.

The molecular systems ppa(H_2O)$_n$ are represented in Fig. 3 in their equilibrium geometries, for n between 1 and 7.

The equilibrium geometries presented in Fig. 3 represent the most stable conformations among those studied, especially for $n>4$, for which more than one isomer are theoretically predicted. In these systems, water molecules interact with the phosphonic acid group as bases or acids. The presence of a basic oxygen atom in P=O with a highly available electronic density is responsible for the interactions where water acts as an acid. The formation of such structures strongly affect the molecular geometry due to the changes in electronic density imposed by the presence of water molecules.

In model systems containing up to 4 water molecules, all of these interact directly with the phosphonic acid group. Systems with $n>4$, however, exhibit ppa$\cdots H_2O\cdots H_2O$ interactions, where some of the water molecules are excluded of the first hydration sphere (h^1), which is formed by four solvent molecules. The formation of an h^1 containing four water molecules is an indicative of the minimum [H_2O]/[PO_3H_2] ratio for which the conductivity is not limited by the number of proton carriers (water molecules acting in the charge transport). For membranes with a [H_2O]/[PO_3H_2] ratio lower than 4, the water

Table 1
Selected geometrical parameters for ppa, (ppa)$_2$(a) and (b)

	ppa	(ppa)$_2$(a)	(ppa)$_2$(b)
d(C–P) (Å)	1.82441	1.82382	1.82062
d(P=O) (Å)	1.49209	1.50749	1.51351
d(P–O) (Å)	1.63226	1.66322/1.57757	1.63263/1.58667
d(O–H) (Å)	0.96879	0.97020/1.02520	0.96830/1.01572
<(O=P–O) (°)	113.370	117.463/108.651	114.586/110.963
<(O–P–O) (°)	104.522	102.445/107.300	107.371

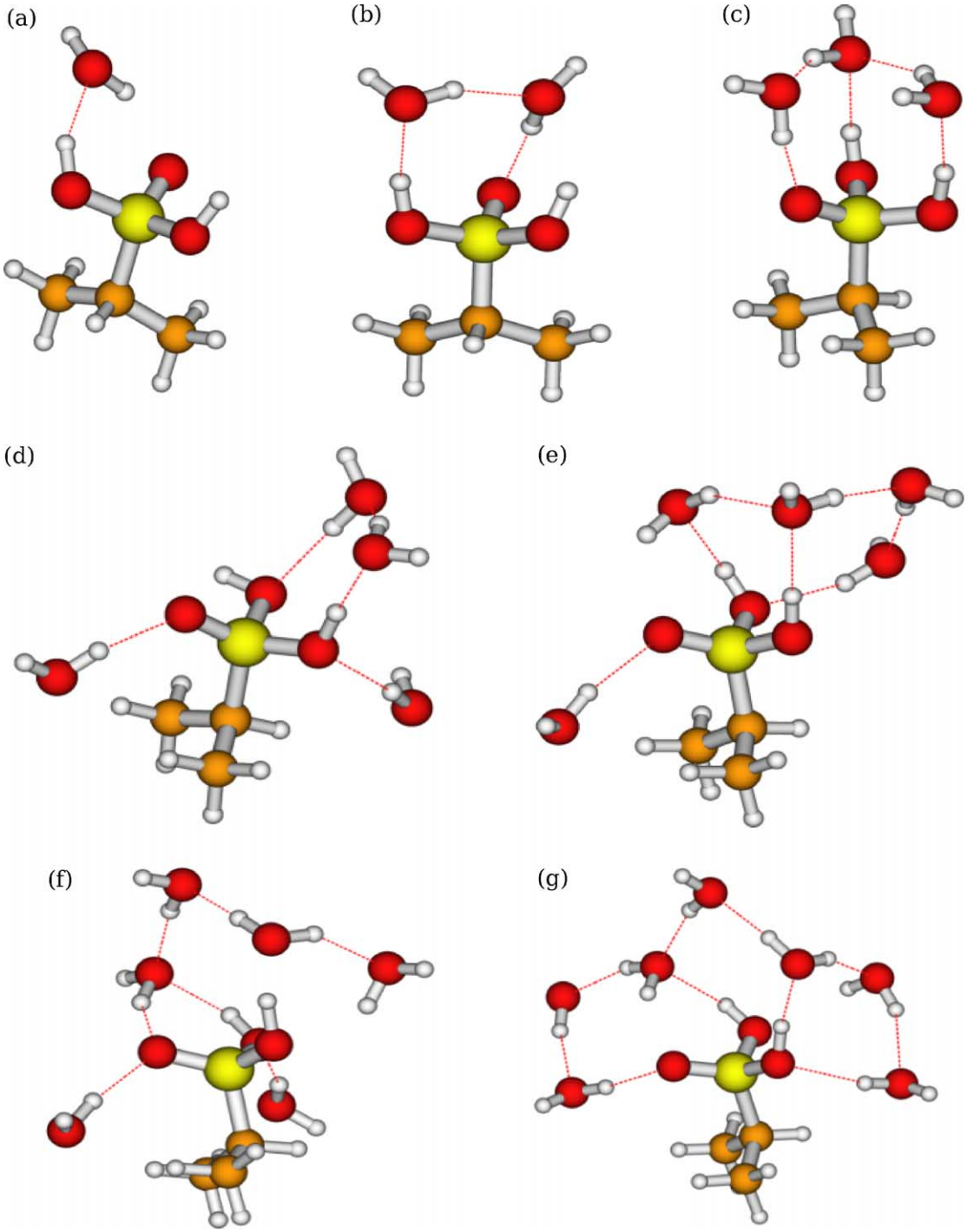

Fig. 3. Molecular structure of model systems describing the hydration sphere of propyl phosphonic acid (ppa$(H_2O)_n$). (a) $n=1$; (b) $n=2$; (c) $n=3$; (d) $n=4$; (e) $n=5$; (f) $n=6$ and (g) $n=7$.

molecules would be strongly bonded to the phosphonic acid group and, therefore, not available for proton transport.

Fig. 4 shows the dependence of P–OH (a), POH···OH_2 and P=O bond lengths with n and Table 2 lists selected geometrical parameters for the ppa$(H_2O)_n$ model systems.

The analysis of the bond lengths as a function of the number of water molecules in the hydration sphere shows that the more significant changes occur in the acid group, as expected. The hydroxyl groups (POH) behave differently from each other, one of them interacting with water as an acid and the other as a base. The OH group acting as an acid is represented by PO–H···OH_2, while the one acting as a base, by PO(–H)···HOH. The bond lengths in both PO–H···OH_2 and PO(–H)···HOH presented a small variation for n between 1 and 4, due to the position of water molecules around the acid group, as observed in Fig. 3(a)–(d).

The water uptake of 6.7% in a poly(styrene–*co*–vinyl phosphonic acid) determined experimentally [23] allowed

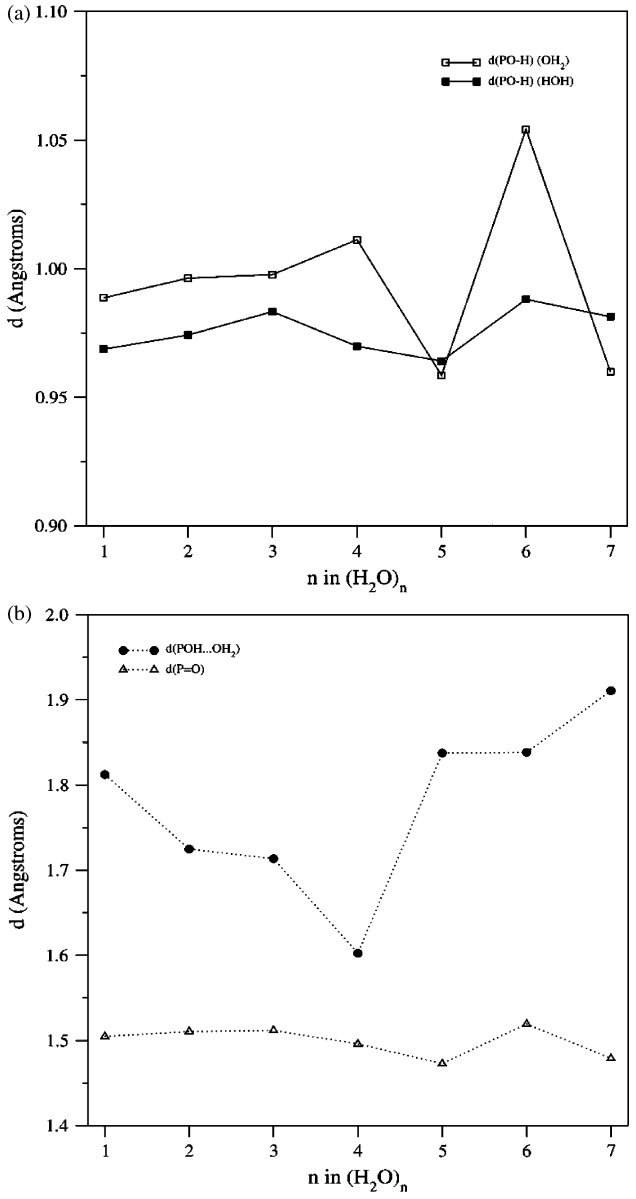

Fig. 4. Dependence of P–OH (a), POH···OH_2 and P=O bond lengths with n.

the calculation of the ratio between the number of water molecules and the number of acid groups in the polymer chain ($[H_2O]/[PO_3H_2]$) as 6.3. The DFT calculations describe the system with a first hydration sphere complete for $n=4$ and for n up to 7, a second hydration sphere is formed. Comparison of experimental and theoretical results indicate the stabilization of the system with the formation of a second hydration sphere.

The formation of a hydration sphere with this number of water molecules in a copolymer with the structural characteristics observed experimentally (styrene:phosphonic acid ratio, polymerization degree) suggests that the hydrophobic fraction of the polymer (the styrene units) does not inhibit the diffusion or arrangement of water molecules around the acid group in the chain.

For a system $P(U_n)$ where U is the fundamental unit and n is the total number of units in the system, the total energy by unit (E/n) can be obtained from

$$\frac{E}{n} = \lim_{n\to\infty} \frac{E\{P(U_n)\}}{n}$$

In the present system, the unit U represents water molecules surrounding the ppa and ppa–H^+ systems and the dependence of the total energy divided by n (E/n) with n for ppa$(H_2O)_n$ and ppa–H^+ $(H_2O)_n$ is shown in Fig. 5. E/n may be interpreted as an energy density for the acid–water interaction, which should converge as n approaches ∞. From Fig. 5, an asymptotic behavior of E/n with n is observed, exhibiting a tendency to converge at -100 hartree/water molecule. For $n=7$, E/n can be considered close to convergence. The approach employed in the present work aims to the description of the hydration sphere around the phosphonic acid group considering explicit water molecules and their interactions via DFT calculations. For n between 6 and 7, the theoretically predicted structure is probably the one present in experimentally hydrated membranes, which allows a molecular interpretation of the water uptake by the system.

The Mülliken charges on the hydrogen and oxygen atoms in ppa and ppa$(H_2O)_n$ model systems are listed in Table 3. A clear electronic density differentiation is observed on both oxygen and hydrogen atoms of the hydroxyl groups for n between 1 and 7, also comparatively to the ppa isolated system. However, the general tendency of the Mülliken charges over the oxygen and hydrogen atoms (of the hydroxyl groups) is that the difference between the two groups progressively decreases, indicating an equivalence in the electronic structure, as well as in the molecular geometry. This electronic balance is induced by a more homogeneous media (with a higher number of water molecules), in which each group is capable of interacting with a large number of solvent molecules. This behavior is thus

Table 2
Selected geometrical parameters for ppa and ppa$(H_2O)_n$

	d(C–P) (Å)	d(P=O) (Å)	d(P–O) (Å)	d(O–H) (Å)	d(POH···OH_2) (Å)
ppa$(H_2O)_1$	1.82304	1.50471	1.61230 (OH_2); 1.62893	0.98866 (OH_2); 0.96870	1.62434
ppa$(H_2O)_2$	1.82009	1.51052	1.60275 (OH_2); 1.62988	0.99633 (OH_2); 0.97421	1.55500
ppa$(H_2O)_3$	1.82131	1.51186	1.60478; 1.61893	0.99770; 0.98330	1.54043
ppa$(H_2O)_4$	1.82521	1.49599	1.67179 (HOH); 1.59729 (OH_2)	0.96987 (HOH); 1.01128 (OH_2)	1.38890
ppa$(H_2O)_5$	1.82035	1.47282	1.59894 (HOH); 1.57970 (OH_2)	0.96393 (HOH); 0.95865 (OH_2)	1.40879
ppa$(H_2O)_6$	1.81987	1.51931	1.63549 (HOH); 1.58387 (OH_2)	0.98808 (HOH); 1.05422 (OH_2)	1.46104
ppa$(H_2O)_7$	1.80426	1.47889	1.57186 (HOH); 1.59006 (OH_2)	0.98135 (HOH); 0.95991 (OH_2)	1.64195
ppa$(H_2O)_{14}$	1.80218	1.50969	1.67089; 1.68110	0.96291; 0.96301	1.77192; 1.80733
ppa$(H_2O)_{28}$	1.79136	1.51033	1.66889; 1.70018	0.96662; 0.96282	1.76886; 1.79759

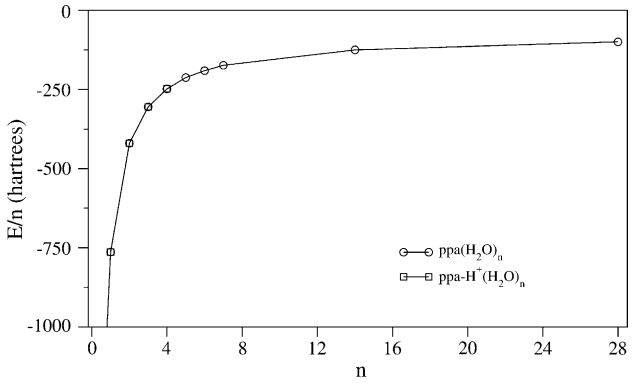

Fig. 5. Dependence of the total energy divided by n (E/n) with n for ppa$(H_2O)_n$ and ppa–$H^+(H_2O)_n$.

confirmed analyzing the model systems containing 14 and 28 water molecules, where the difference in the Mülliken charges for the equivalent atom are almost negligible.

In Fig. 6, the molecular structure of ppa$(H_2O)_{14}$ and ppa$(H_2O)_{28}$ are shown, as obtained only for comparison of the total energy divided by the number of water molecules in the system. These structures obtained from geometry optimization with a 3-21G basis set are not suitable for fine comparisons with the ppa$(H_2O)_n$ series (n from 1 to 7), but indicate that the inner hydration sphere formed with n up to 7 keeps its structure even for 14 or 28 water molecules. As expected, water molecules in these structures tend to avoid the $–CH_3$ groups, preferentially forming an arrangement around the phosphonic acid group and, for n higher than 7, around other water molecules already placed in the hydration sphere. Despite the different basis sets employed in the calculations for $n=1$–7 (6-31G(d,p)) and $n=14$ or 28 (3-21G), some interesting structural characteristics can be noted, observing the data listed in Table 2. The carbon–phosphorous bond length apparently tends to decrease with n, as noted for n between 1 and 7 also confirmed for 14 and 28 water molecules in the hydration sphere. The phosphorous–oxygen bond lengths (both P–O and P=O) are strongly influenced by the number of water molecules interacting with each center, the geometry of the interaction and its nature (if water acts as acid or base). An oscillatory behavior with n is associated with local changes in the molecular structure of the model systems, which is a reflect of the changes in the electronic structure, specially for the

Table 3
Mülliken charges on the hydrogen and oxygen atoms in ppa and ppa$(H_2O)_n$ model systems

	(PO)H	(P)O	(P=)O
ppa	0.4164	−0.1596	−0.0645
ppa$(H_2O)_1$	0.4075; 0.4284	−0.1528; −0.1721	−0.0105
ppa$(H_2O)_2$	0.4010; 0.4218	−0.1586; −0.1811	−0.0175
ppa$(H_2O)_3$	0.4098; 0.4190	−0.1610; −0.1735	−0.0236
ppa$(H_2O)_4$	0.3749; 0.4134	−0.1727; −0.2314	−0.0088
ppa$(H_2O)_5$	0.4080; 0.4120	−0.1842; −0.2158	−0.0169
ppa$(H_2O)_6$	0.3981; 0.4083	−0.1610; −0.2164	−0.0673
ppa$(H_2O)_7$	0.3993; 0.4156	−0.1873; −0.2058	−0.0323
ppa$(H_2O)_{14}$	0.3957; 0.3956	−0.2263; −0.2335	−0.0760
ppa$(H_2O)_{28}$	0.3888; 0.3923	−0.2319; −0.2693	−0.0779

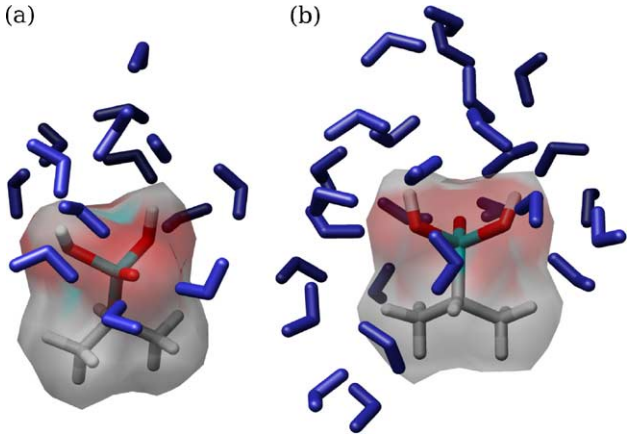

Fig. 6. Molecular structure of ppa$(H_2O)_{14}$ (a) and ppa$(H_2O)_{28}$ (b).

specific, highly localized water–phosphonic acid interactions in the present system. The O–H (hydroxyl) bond lengths in ppa$(H_2O)_{14}$ and ppa$(H_2O)_{28}$ model systems presented an increase relative to $n=1$–7, which is related to the basis set employed in these calculations (3-21G), but also is a result of the higher number of water molecules interacting with the phosphonic acid group. The E/n values for $n=14$ and 28, as observed in Fig. 5, present an excellent agreement with the asymptotic behavior already described for n between 1 and 7. This is due to the magnitude of the stabilization energy originated from the water–water interactions, which does not influence significantly on the total energy for n higher than 7.

3.3. Proton–ppa interactions in ppa–$H^+(H_2O)_n$ systems

Beyond the ppa$(H_2O)_n$ interactions, the description of the molecular interactions in ppa–$H^+(H_2O)_n$ systems is crucial to understand the behavior and structure of the membrane under operational conditions in a PEMFC. In PEMFC, the membrane acts as a proton-exchange medium, where inorganic acids are usually dissolved aiming to increase the number of charge carriers in the solid. In Fig. 7 the molecular structure of ppa–$H^+(H_2O)_n$ model systems with n between 1 and 4 are shown in equilibrium geometries.

From the molecular structures depicted in Fig. 7, expressive changes in the model systems can be observed as the water molecules are added to the hydration sphere of ppa–H^+. It is important to note that the proton is located invariably on the phosphonic acid group, instead of forming a hydronium ($H^+(H_2O)_n$) complex isolated from the ppa molecule. The P=O original bond is then used to form the $(CH_3)_2CHPO_3H_3^+$ protonated acid. This originally basic site (in both isolated and hydrated forms) turns into an additional acid site. Selected bond lengths are listed in Table 4 for the model systems ppa and ppa–$H^+(H_2O)_n$.

Fig. 5 also shows the dependence of E/n with n for the ppa–$H^+(H_2O)_n$ model systems. An asymptotic behavior can be observed, similarly to that of the ppa$(H_2O)_n$ systems. A comparison of the E/n for ppa–$H^+(H_2O)_n$ and ppa$(H_2O)_n$ shows not only similar trends but also very close values, with a negligible difference for systems with $n=4$ or higher.

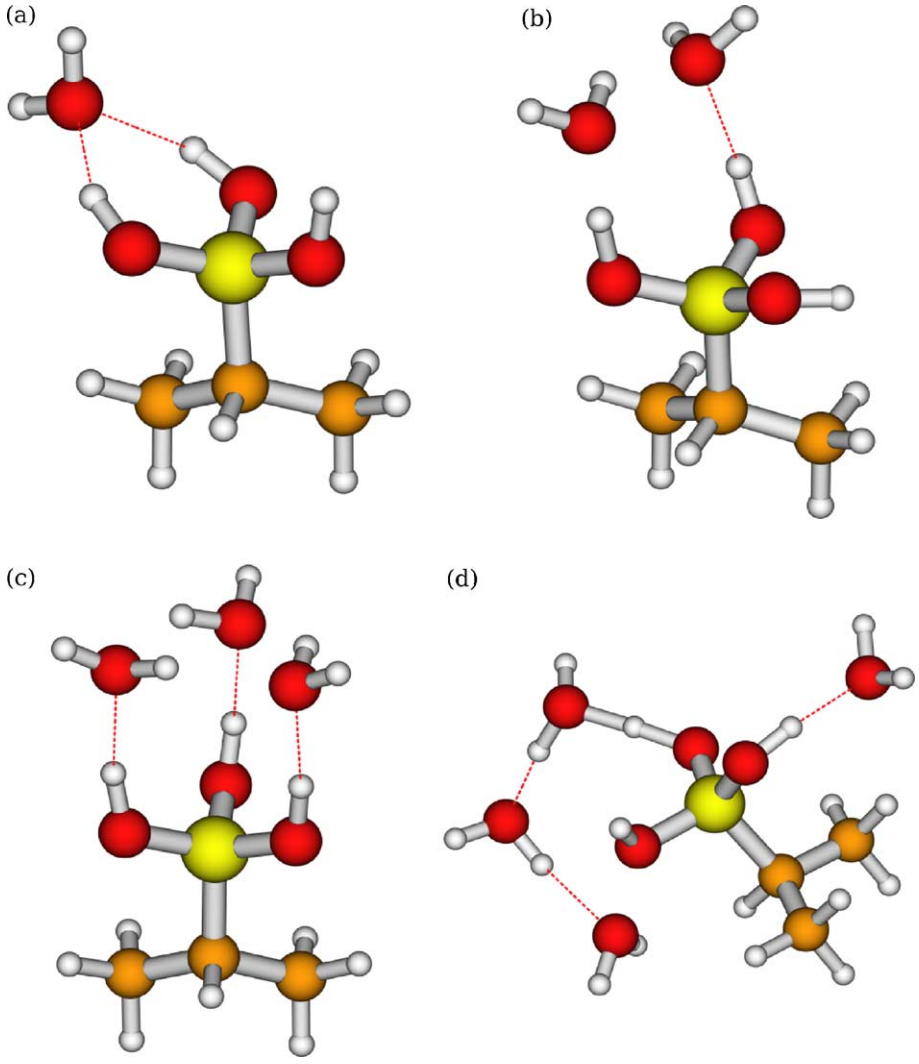

Fig. 7. Molecular structure of ppa–$H^+(H_2O)_n$ model systems with (a) $n=1$; (b) $n=2$; (c) $n=3$; (d) $n=4$.

The convergence of the energy density indicates that, despite the differences in molecular geometry and wavefunction of the two systems, the energy barrier for the formation of protonated species should be small, which influences directly on the experimental features of the phosphonic acid polymeric membrane.

The structural changes induced in the phosphonic acid group by the presence of H^+ are comparatively more expressive than in ppa$(H_2O)_n$ systems, as listed in Tables 2 and 4. The most significant structural changes in ppa–$H^+(H_2O)_n$ with n take place in O–H bond lengths and a small differentiation among the OH groups is observed. These groups should be equivalent in a highly symmetric model but, without geometrical constrains in the geometry optimization calculations, the molecular structure achieves a less symmetric state with higher stability. The analysis of the electronic structure of ppa–$H^+(H_2O)_n$ systems, as well as the molecular geometry, exhibits a decrease in the electronic density between O and H in the three hydroxyl groups depending, however, on the distance between these and the nearest water molecule in the hydration sphere. The phosphorous–oxygen bonds in ppa–$H^+(H_2O)_n$, differently from the O–H, present a decrease of about 5%, indicating an increase in the electronic density between P and O. This is due to a redistribution of electronic density, originally localized in the P=O bond, which presents a bond length d(P=O) = 1.49209 Å in isolated ppa. This electronic density is found distributed among the three P–O bonds, which causes the observed feature. Formation of

Table 4
Selected bond lengths for ppa and ppa–$H^+(H_2O)_n$

	ppa	$n=1$	$n=2$	$n=3$	$n=4$
d(C–P) (Å)	1.82441	1.80032	1.80388	1.79832	1.81185
d(P–O) (Å)	1.63226	1.58087; 1.58604	1.55219; 1.60171	1.58143	1.53684; 1.60578
d(O–H) (Å)	0.96879	0.97109; 0.98597	0.96976; 1.03548	0.99688	0.97008; 1.00850; 1.14876

Table 5
Mülliken charges on the hydrogen and oxygen atoms in ppa and ppa–$H^+(H_2O)_n$ model systems

	ppa	ppa–$H^+(H_2O)_1$	ppa–$H^+(H_2O)_2$	ppa–$H^+(H_2O)_3$	ppa–$H^+(H_2O)_4$
(PO)H	0.4164	0.3541	0.3646	0.3984	0.3887
(PO)H	0.4164	0.3998	0.4001	0.3991	0.3993
(PO)H	–	0.4062	0.4167	0.4001	0.4076
(Water)H	–	0.3431	0.3804	0.3077; 0.3445[a]	0.3224; 0.3590[a]
(P)O	−0.1596	−0.1619	−0.1243	−0.1592	−0.1516
(P)O	−0.1596	−0.1828	−0.1587	−0.1609	−0.1604
(P)O	−0.0645[b]	−0.1773	−0.1669	−0.1617	−0.1723
(Water)O	–	−0.6238	−0.6449	−0.6569	−0.6634

[a] H in hydrogen bond with one water molecule.
[b] P=O bond.

$[R_2CHPO_3H_3]^+$, with three equivalent hydroxyl groups is the main factor to the strong structural changes observed, in comparison with both ppa isolated and in interacting systems with water.

In Table 5, Mülliken charges on the hydrogen and oxygen atoms in ppa and ppa–$H^+(H_2O)_n$ model systems are listed for n between 1 and 4.

From the data in Tables 4 and 5, hydrogen atoms (in POH groups) are found to be equivalent not only structurally, but also in electronic density. In a conventional vehicular mechanism of proton conduction, hydronium $[H(H_2O)_n]^+$ ions should be formed separately (from the phosphonic acid group in the polymer chain), which does not seem to occur in the present system. According to the current vehicular mechanisms described in the literature, these hydronium ions would be carried and, consequently, the charge transport takes place. However, the molecular structure proposed in the present work for a hydrated phosphonic acid-based membrane containing an inorganic acid (such as H_3PO_4) is $[R_2CHPO_3H_3]^+(H_2O)_n$, where formation of a hydronium ion is not observed. These characteristics suggests that a conventional vehicular mechanism is not probable for the present system.

The experimental consequences of the molecular structure described in the present work are not fully clear, but the formation of a protonated acid such as $[R_2CHPO_3H_3]^+$ in the backbone of the polymer chain may be an advantage in the application of a polymeric membrane formed by a copolymer of vinyl phosphonic acid where an inorganic acid (e.g. H_3PO_4) is dissolved acting as proton source to the phosphonic groups in the polymer chain.

Proton transfer in membranes such as NAFION® or poly(ether ether ketone) [24,25], as well as in composite membranes [26] is promoted by the presence of water. The transport mechanisms proposed in the literature for various electrolytes include a vehicular description, where the proton forms a water complex which diffuses through the hydrated membrane [27]. Thus, without the presence of water in conventional membranes, the proton conductivity takes place with a non-vehicular mechanism, such as in poly(benzimidazole)/H_3PO_4 [28]. The proton transport in dry membranes is usually described as a hopping mechanism where the charge carriers move from a basic coordination site to the next one. These sites are usually immobilized in the polymer chain, as in poly(imidazole) and poly(benzimidazole) [29]. The proton conduction models reported in the literature usually involve thermodynamic descriptions [30], which consist in macroscopic approaches to the interpretation of the conductivity behavior observed in polymeric membranes. These mechanisms include proton diffusion (at low temperatures) or migration (at high temperatures) [31]. At low temperatures, proton transport is influenced by viscosity since both transport and viscosity involve intermolecular interactions, especially hydrogen bonding. As temperature increases, the local order is reduced due to Brownian motion and the clusters originally formed by hydrogen bonding interaction are broken, inducing a change in the conduction mechanism. In the present work, however, the proton equivalence in ppa–$H^+(H_2O)_n$ model systems indicates that conventional vehicular mechanisms are unlikely in the present system, for which a charge localization would be expected in a particular hydrogen atom, as well as the formation of hydronium $H^+(H_2O)_n$ species. The general formula $[R_2CHPO_3H_3(H_2O)_n]^+$ is proposed as representative of phosphonic acid-based polymer molecular structure in acid (hydrated) conditions.

4. Conclusions

In the present work, both the molecular and electronic structures of ppa were described by means of theoretical calculations based on the density functional theory. The formation of ppa dimers was reported and a not negligible energetic difference between the two dimer structures was found in the gas phase.

The hydration sphere of ppa was built by adding water molecules around the phosphonic acid group and further geometry optimization. The model system ppa$(H_2O)_n$ with $n=4$ formed the first hydration sphere (h^1), while $n=7$ can be considered a good approximation to the complete inner hydration sphere around the phosphonic acid group. This assumption is strongly supported by the asymptotic behavior of the E/n values and the structures with 14 and 28 water molecules, which shows little or none variation for the inner hydration sphere with the addition of more water molecules.

The study of the ppa–$H^+(H_2O)_n$ model systems showed an interesting structural behavior comparatively to the ppa $(H_2O)_n$ systems. The protonated acids exhibited equivalent phosphorous–oxygen bonds and a general molecular structure

$[R_2CHPO_3H_3(H_2O)_n]^+$ is proposed to represent these protonated species.

Acknowledgements

Authors would like to thank CNPq for fellowships and support of the present work (CNPq/CT/Energ Nos 50.4222/2004-0 and 40.1494/2003-9) and FAPERJ (E-26/170.700/2004).

References

[1] Kobayashi T, Rikukawa M, Sanui K, Ogata N. Solid State Ionics 1998; 106:219.
[2] Acres GJK, Frost JC, Hards GA, Potter RJ, Ralph TR, Thompsett D, et al. Catal Today 1997;38:393.
[3] Smitha B, Sridhar S, Khan AA. J Membr Sci 2005;259:10.
[4] Seeliger D, Harting C, Spohr E. Electrochim Acta 2005;50:4234.
[5] Slade RCT, Varcoe JR. Solid State Ionics 2005;176:585.
[6] Randin J-P. J Electroanal Chem 1982;129:1215.
[7] Poltarzewski Z, Wiekzorek W, Przyluski J, Antonucci V. Solid State Ionics 1999;119:301.
[8] Kordesch KV, Simader GR. Chem Rev 1995;95:191.
[9] Savienell RF, Yeager E, Tryk D, Landau U, Wainright JS, Weng D, et al. J Electrochem Soc 1994;141:146.
[10] Haubold H-G, Vad Th, Jungbluth H, Hiller P. Eletrochim Acta 2001;46: 1559.
[11] Paddison SJ, Elliott JA. J Phys Chem A 2005;109:7583.
[12] Kreuer KD, Paddison SJ, Spohr E, Schuster M. Chem Rev 2004;104: 4637.
[13] Rivas BL, Pereira E, Gallegos P, Homper D, Geckeler KE. J Appl Polym Sci 2004;92:2917–22.
[14] Smitha B, Shridar S, Khan AA. J Membr Sci 2005;259:10–26.
[15] Wu Q, Weiss RA. J Polym Sci, Part B: Polym Phys 2004;42:3628–41.
[16] Becke AD. J Chem Phys 1993;98:5648.
[17] Schmidt MW, Baidridge KK, Boatz JA, Elbert ST, Gordon MS, Jensen JH, et al. J Comput Chem 1993;14:1347.
[18] Weakley TJR. Acta Crystallogr B 1976;32:2889.
[19] Hernández-Laguna A, Sainz-Díaz CI, Smeyers YG, de Paz JLG, Gálvez-Ruano E. J Phys Chem 1998;98:1109.
[20] Pereira RP, Rocco AM, Bielschowsky CE. J Phys Chem B 2004;108: 12677 [and references cited].
[21] Glukhovtsev MN, Bach RD, Nagel CJ. J Phys Chem A 1997;101:316.
[22] Zhang Y, Zhao J, Tang G, Zhu L. Spectrochim Acta Part A 2005;62:1.
[23] Rocco AM, Felisberti MI, Girão LFC, Viol JB, Pereira RP. Submitted for publication.
[24] Rikukawa M, Sauni K. Prog Polym Sci 2000;25:1463.
[25] Kerres JE. J Membr Sci 2001;185:29.
[26] Nakajima H, Honma I. Solid State Ionics 2002;148:607.
[27] Navarra MA, Panero S, Scrosati B. J Solid State Electrochem 2004;8:804.
[28] Yamada M, Honma I. Polymer 2005;46:2986.
[29] Münch W, Kreuer K-D, Silvestri W, Maier J, Seifert G. Solid State Ionics 2001;145:437.
[30] Elabd YA, Napadensky E, Sloan JM, Crawford DM, Walker CW. J Membr Sci 2003;217:227.
[31] Schechter A, Savinell RF. Solid State Ionics 2002;147:181.